5th International Science Congress & Exhibition APMAS2015, Lykia, Oludeniz, April 16–19, 2015

Electrochemical Characterization of Al^{3+} Doped Spinel Cathode Active Nanoparticles for Li-Ion Batteries

E. Bulut[a,*], M. Can[b], M. Özacar[a] and H. Akbulut[c]

[a]Sakarya University, Chemistry Department, 54187, Sakarya, Turkey

[b]Sakarya University, Vocational School of Arifiye, 54580, Arifiye, Sakarya, Turkey

[c]Sakarya University, Metallurgical and Materials Engineering, 54187, Sakarya, Turkey

Al^{3+} doped spinel structured cathode active nanoparticles were produced by microwave hydrothermal synthesis. Structural characterization of as synthesized nanoparticles was performed by X-Ray Diffraction (XRD) Spectroscopy and Scanning Electron Microscopy (SEM). Electrochemical characteristics of the material have been investigated by packaging cell material into a CR 2016 button cells. All electrochemical experiments were carried out using lithium metal foil as the counter electrode. First discharge capacitiy of doped material is 303 mAh/g at 0.1 C rate. We have obtained 69 mAh/g specific capacity and 98.7 percent capacity retention for the first cycle at 0.5 C rate.

DOI: 10.12693/APhysPolA.129.631

PACS/topics: 82.47.Aa

1. Introduction

The capacity fading that occurs in $LiMn_2O_4$ is due the structural transformation from cubic to tetragonal phase with cycling. This structural transformation is due to the Mn^{3+} ($3d^4$). Capacity fading is also caused by lattice instability, manganese dissolution, oxidation of the electrolyte, formation of oxygen rich spinel and particle disruption [1–3]. Several studies have been conducted to enhance the cyclic performance of $LiMn_2O_4$ at room temperature by the partial substitution of Mn^{3+} in $LiMn_2O_4$ with other trivalent cations (e.g. Fe, Al, Cr) or divalent cations (e.g. Zn, Ni, Mg), because it reduces the Mn^{3+} content and stabilizes the cubic structure of the spinel [4–7].

$LiMn_2O_4$ spinel was traditionally prepared by solid-state reaction directly at high temperatures [8, 9]. In recent years, nanostructures have received intensive attention because of both their fundamental importance and the wide range of their potential applications in many areas. Most of the nanostructured electrode materials are synthesized by the low-temperature treatment processes such as soft chemical [10], sol-gel [11], Pechini process [12] microwave synthesis route [13] and hydrothermal methods [14]. The hydrothermal synthesis can control the particle size and the crystalline nature of the product. Also hydrothermal method enables to synthesize materials at a lower temperature than the conventional solid state route.

In the present work, we first aimed to synthesize Al^{3+} doped spinel $LiAl_{0.02}Mn_{1.98}O_4$ cathode active nanoparticles by microwave hydrothermal method to enhance the electrochemical performance of the spinel cathode active materials. However, we have noticed other phases, (Li_2MnO_3 and spinel $Li_{1.27}Mn_{1.73}O_4$ with excess Li). Then efficiency of these phases in the electrochemical performance was investigated and an enhanced specific capacity was obtained. The specific capacities of first discharges are higher than theoretical and literature values [15, 16]. Cathode active nanoparticles were easily produced using microwave irradiation and were characterized structurally and electrochemically.

2. Materials and methods

In this study we present the preparation and characterization of aluminum (Al^{3+}) doped $LiMn_2O_4$ spinel cathode active nanoparticles by microwave assisted hydrothermal method to improve electrochemical features of Li-ion cells. In a typical process, stoichiometric amounts of $LiNO_3$, $Mn(CH_3COO)_2$, $Al(NO_3)_3{\cdot}9H_2O$ were dissolved in distilled water. The resulting solution was magnetically stirred and then was transferred into a teflon-lined autoclave. The tightly sealed autoclave was kept at 160 °C for 1 hour in a microwave oven. After the hydrothermal treatment, the products dried in air at 105 °C for 12 hours. The final product, $LiAl_{0.02}Mn_{1.98}O_4$ nanoparticles, were obtained by calcination in a muffle furnace at temperatures of 500 and 700 °C for 6 hours in air.

The powder structure and morphology investigation of the as-synthesized $LiAl_{0.02}Mn_{1.98}O_4$ nanoparticles at different calcination temperatures were performed by XRD (RIGAKU D max 2200) and SEM (JEOL JSM-6060 LV) respectively. Lattice parameters of the spinel structured compounds were calculated from the XRD data using Williamson-Hall equation [17].

*corresponding author; e-mail: ebulut@sakarya.edu.tr

CR 2016 button cells were produced for electrochemical characterization. Electrode material was prepared by thoroughly mixing 76 wt.% cathode active material $LiAl_{0.02}Mn_{1.98}O_4$, 9 wt.% acetylene black and 15 wt.% Polyvinylidene fluoride (PVDF) using N,N-Dimethylformamide (DMF) to form a homogeneous slurry, which was spread on Al foil and dried at 120 °C under vacuum for 12 hours. The cell construction and sealing were carried out in an argon-filled glove box (M Braun Model Unilab). Li foils were used as anode. A microporous polypropylene film was used as separator between electrodes. The electrolyte was a 1 M $LiPF_6$ solution in Ethylene Carbonate-Dimethyl Carbonate (EC-DMC, 1:1 in volume) soaked in a polyethylene separator. The galvanostatic cycling tests were carried out with a MTI Battery tester using CR 2016 button cells. The initial charge and discharge tests were carried out at a constant current density over the potential range of 3–5 V vs. Li/Li^+.

3. Results and discussion

The powder XRD patterns of $LiAl_{0.02}Mn_{1.98}O_4$ materials calcined at different temperatures are shown in Fig. 1. All samples were identified as spinel structures with a cubic unit cell and Fd3m space group. Also, some additional small peaks of impurity phases were observed at about $2\theta = 23°$, 33°, 55°, 37° and 45°, which are attributed to the formation of Mn_2O_3 and Li_2MnO_3 respectively.

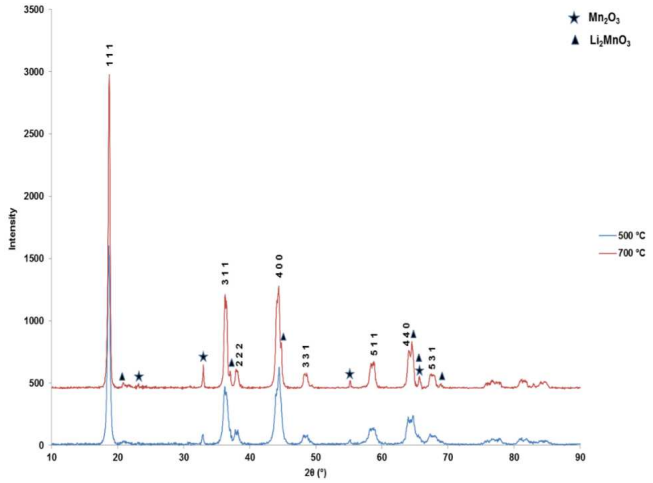

Fig. 1. XRD patterns of $LiAl_{0.02}Mn_{1.98}O_4$ cathode active materials.

Also when we zoom into the XRD pattern, Li-excessive $Li_{1.27}Mn_{1.73}O_4$ phase was becoming visible. Essentially, poliphasic cathode active materials were formed with tree integrated phases of $LiAl_{0.02}Mn_{1.98}O_4$, Li_2MnO_3, $Li_{1.27}Mn_{1.73}O_4$ at 500 °C. When the calcination temperature was set to 700 °C, the well-crystallized spinel compound was obtained. Heating to higher temperatures resulted in an increase in the crystallinity of $LiAl_{0.02}Mn_{1.98}O_4$ [18]. Calculated lattice parameters are 8.166 and 8.196 Å for samples calcinated at 500 and 700 °C, respectively. It is confirmed that the incorporation of Al^{3+} into the spinel lattice should result in the decrease in quantity of the larger Mn^{3+} ions, decrease of the lattice parameter and also in shrinkage of unit cell volume. This could restrain the spinel structural change and stabilize spinel structure during cycling.

Since surface morphology is also an important factor for the cathode active materials due to cycling performance, it was studied by SEM and FESEM for all doped and undoped spinels investigated in this work. Figure 2 shows typical SEM images of doped materials. In all cases, grains of similar forms and highly uniform size distribution were observed. The average grain size was about 50 nm for 500 °C.

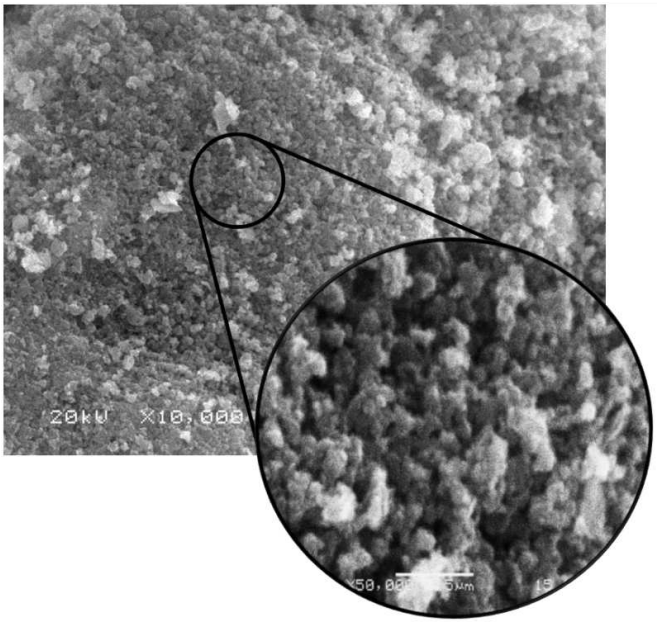

Fig. 2. Typical SEM images of $LiAl_{0.02}Mn_{1.98}O_4$. Magnification of inner image is ×50000.

The electrochemical features of as-synthesized $LiAl_{0.02}Mn_{1.98}O_4$ nanoparticles calcined at 500 °C were examined using $Li//LiAl_{0.02}Mn_{1.98}O_4$ cells. As-prepared CR2016 button cells were submitted to constant current cycling under galvanostatic conditions at 25 °C. The first discharge characteristics of electrochemical $Li//LiAl_{0.02}Mn_{1.98}O_4$ cells measured at 0.1 C rates, while the voltage was monitored between 3 and 5 V, are presented in Fig. 3.

First discharge capacitiy of doped material is 303 mAh/g. The specific capacities of first discharges are higher than theoretical and literature values. Smaller size and better distribution of cathode active nanoparticles could be possibly responsible for the increase in the specific capacity. In fact shape of the charge/discharge curve shows the layered-spinel-Li rich spinel three integrated phase

composite electrodes (Li_2MnO_3, $LiAl_{0.02}Mn_{1.98}O_4$, $Li_{1.27}Mn_{1.73}O_4$). The 3.3 V plateau is a characteristics of the Li-rich spinel phase, $Li_{1.27}Mn_{1.73}O_4$. However the characteristic voltage plateaus of spinel (3.9–4.1 V) were shifted to 4.3–4.5 V range due to this lithium substituted spinel. In addition to these, two phases (spinel+Li-excess spinel) mentioned above, it has already been established that extra charging capacity beyond the limit based on the tetravalent transition metals is closely related to the characteristic feature of Li_2MnO_3, due to possible simultaneous removal of lithium and oxide ions [19].

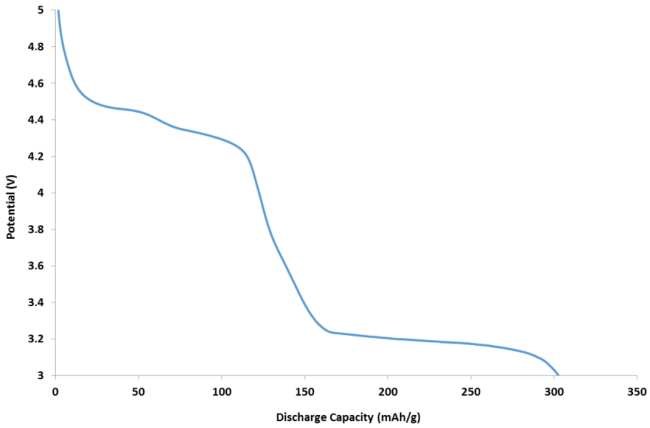

Fig. 3. First discharge plot of $LiAl_{0.02}Mn_{1.98}O_4$ cathode active nanoparticles at 0.1 C rate.

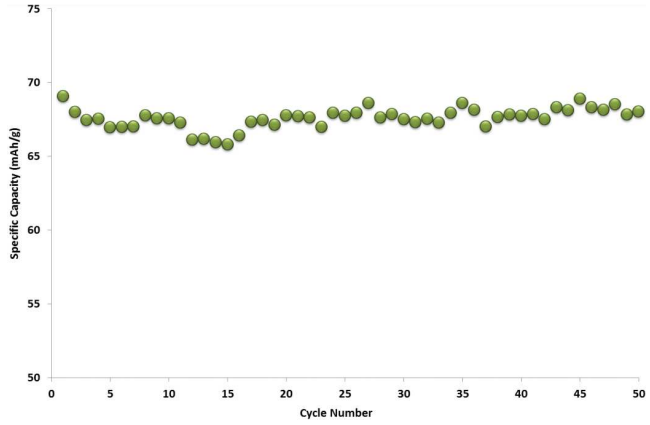

Fig. 4. Specific capacity at 0.5 C rate as a function of cycle number, obtained during charge and discharge tests.

The cycling performance of the sample at the current rate of 0.5 C is shown in Fig. 4. Relatively low conductivity of Li excess spinels, exists in the material, restricting its high-rate performance. Li^+ ions are agglomerated on surfaces of the nanoparticles during high-rate discharge due to this low conductivity. And this fact gradually deteriorates electrochemical performance [20]. Therefore we obtained lower capacities at 0.5 C rate than the ones obtained at 0.1 C rate. As-synthesized material delivers initial discharge capacity of 69 mAh/g; and after 50 cycles, the capacity decreases to 68 mAh/g with 98.7% capacity retention. The results of the galvanostatic discharge indicate that the doping could effectively improve the cycling performance of the spinel $LiMn_2O_4$. Metal-ion substitution could improve the stability of the spinel structure and suppress the Mn dissolution. Obviously, incorporation of Al^{3+} into the spinel lattice improves the cyclability.

4. Conclusions

All observed types of particles are well crystallized, with their sizes ranging from 50 nm to 200 nm depending on the calcination temperature. Particles calcined at 500 °C are about 50 nm in size, have hexagonal shapes and a uniform size distribution. For the present work, we have concentrated on the charge-discharge characteristics in 3–5 V (4 V range) and 3–4.3 V regime, where apparently, the J-T distortion should not affect the cycleability of the cathode materials. We have achieved 69 mAh/g capacity for the first cycle and 68 mAh/g specific capacity after 50 cycles at 0.5 C rate. The obtained capacity retention is 98.7% throughout 50 cycles and the coulombic efficiency per cycle is above 95%. While considering the cycling stability and coulombic efficiency, low-level doping is found to be beneficial.

Acknowledgments

This project is financially supported by Sakarya University, Scientific Research Project Commission under grant of 2014-02-04-001.

References

[1] A. Yamada, *J. Solid State Chem.* **122**, 160 (1996).

[2] Y. Gao, J.R. Dahn, *Solid State Ionics* **84**, 33 (1996).

[3] S.T. Myung, H.T. Chung, S. Komaba, N. Kumagai, H.B. Gu, *J. Power Sources* **90**, 103 (2000).

[4] Q. Feng, H. Kanoh, Y. Miyai, K. Ooi, *Chem. Mater.* **7**, 379 (1995).

[5] T. Nakamura, H. Demidzu, Y. Yamada, *J. Phys. Chem. Solids.* **69**, 2349 (2008).

[6] X. Wang, O. Tanaike, M. Kodama, H. Hatori, *J. Power Sources* **168**, 282 (2007).

[7] F.A. Amaral, N. Bocchi, R.F. Brocenschi, S.R. Biaggio, R.C. Rocha-Filho, *J. Power Sources* **195**, 3293 (2010).

[8] T. Kakuda, K. Uematsu, K. Toda, M. Sato, *J. Power Sources* **167**, 499 (2007).

[9] J.M. Tarascon, E. Wang, F. Shokoohi, W.R. Makinnon, S. Colson, *J. Electrochem. Soc.* **138**, 2859 (1991).

[10] J. Luo, Y. Wang, H. Xiong, Y. Xia, *Chem. Mater.* **19**, 4791 (2007).

[11] X. Li, R. Xiang, T. Su, Y. Qian, *Mater. Lett.* **61**, 3597 (2007).

[12] Y.S. Han, H.G. Kim, *J. Power Sources* **88**, 161 (2000).

[13] P. Ragupathy, H.N. Vasan, N. Munichandraiah, *Mater. Chem. Phys.* **124**, 870 (2010).

[14] H. Yue, X.K. Huang, D.P. Lv, Y. Yang, *Electrochim. Acta* **54**, 5363 (2009).

[15] S. Nieto, S.B. Majumder, R.S. Katiyar, *J. Power Sources* **136**, 88 (2004).

[16] Y.S. Lee, N. Kumada, M. Yoshio, *J. Power Sources* **96**, 376 (2001).

[17] E. Bulut, Ph.D. Thesis, Sakarya Üniversitesi Fen Bilimleri Enstitüsü, Sakarya, 2013.

[18] E. Bulut, A. Örnek, M. Özcar, *Adv. Sci. Eng. Med.* **3**, 67 (2011).

[19] N. Yabuuchi, K. Yoshii, S.T. Myung, I. Nakai, S. Komaba, *J. Am. Chem. Soc.* **133**, 4404 (2011).

[20] H. Wang, T.A. Tan, P. Yang, M.O. Lai, L. Lu, *J. Phys. Chem. C.* **115**, 6102 (2011).